PROCEEDINGS, Thirty-Sixth Workshop on Geothermal Reservoir Engineering
Stanford University, Stanford, California, January 30 - February 1, 2012
SGP-TR-194

NATURAL RESERVOIR EVOLUTION IN THE TOLHUACA GEOTHERMAL FIELD, SOUTHERN CHILE

Glenn Melosh[1], Joseph Moore[2], and Robert Stacey[1]
[1]GeoGlobal Energy, 115 4th St., Santa Rosa, CA, 95409, USA
gmelosh@gmail.com

[2]Energy & Geoscience Institute at the University of Utah, 423 Wakara Way, Salt Lake City, Utah, 84108, USA

ABSTRACT

The Tolhuaca geothermal reservoir formed as a liquid-dominated hydrothermal system in a topographically-elevated young volcanic rift zone on the flank of Tolhuaca stratovolcano. Early shallow upflow established temperatures near boiling in a roughly horizontal liquid reservoir zone at 100 to 200 m depth. The shallow high temperatures eventually supported hydrothermal brecciation – boiling events that penetrated into a deeper reservoir to at least 950 m depth. Boiling was followed by steam-heated water invasion that cooled the reservoir. The latest stage has involved reservoir reheating and boiling to create a system with deep hot brine below a separate shallow steam zone. An upflow conduit that links and supports these two zones has been interpreted based on the presence of a resistive zone related to relatively high temperature mineralization. Well temperatures nearby suggest that the upflow is currently steam-dominated down to 600 m depth. The reservoir zones are overlain by steam-heated water. The top of the shallow steam zone appears to be controlled by quenching by steam-heated water. This model is supported by surface mapping, fluid geochemistry, geophysics, core and cuttings mineralogy, rock isotopes, fluid inclusions, local hydrology, well temperatures and well testing. These data provide an unusually detailed model of reservoir evolution in a field with just two slim wells and a deep well in progress.

INTRODUCTION

The Tolhuaca geothermal field lies along a NW trend of young volcanoes in the Southern Volcanic Zone of the Andes in Chile about 600 km south of Santiago (Figure 1). Proceeding from the southeastern end of the trend, the volcanism includes Lonquimay and Tolhuaca stratovolcanoes and the Pemehue volcanic trend on the northwestern flank of Tolhuaca. The Pemehue area has experienced very young northwest-trending basaltic rift eruptions, cone formation, and flows. The youngest Pemehue area volcanism includes post-glacial flows that are dated to be less than 6000 years old (J. A. Naranjo, pers. com., 2010).

The geothermal prospect was identified from three fumarole areas spaced along 2.5 km of the Pemehue volcanic trend along with surface alteration and numerous steam-heated hot springs (Figure 2). The exploration process has included geologic, geochemical, and geophysical surveys and the drilling of two slim wells to 1073 m (Tol-1) and 1274 m (Tol-2) depth. A deep full-size exploration well has recently been completed. This report summarizes aspects of various data sets and then pulls them together into a conceptual model of the reservoir evolution.

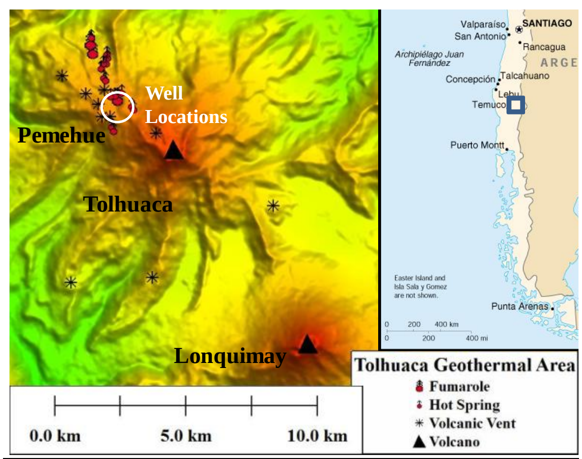

Figure 1: The Tolhuaca Geothermal Field is located on the northwest flank of Tolhuaca Volcano in Southern Chile.

SURFACE HYDROTHERMAL FEATURES

The thermal features lie along the Pemehue volcanic trend (Figure 2). In addition to the three fumaroles, 17 steam-heated bicarbonate hot springs with temperatures ranging from 20 to 60°C are scattered along the trend.

Surface hydrothermal alteration shows widespread acid-sulfate style mineralization toward the summit of Tolhuaca Volcano. Argillic alteration is scattered at the surface in the main part of the geothermal prospect as confirmed by X-ray diffraction (XRD) and infra-red hyperspectral analyses of surface samples. Three silica sinter terraces and numerous more limited surficial silica deposits occur along the trend (Figure 2).

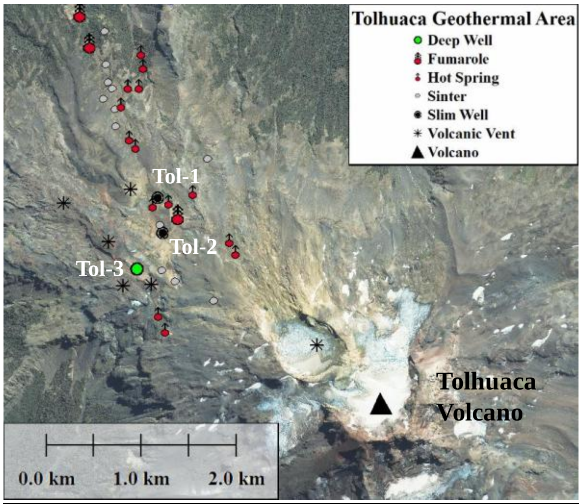

Figure 2: Ikonos image showing thermal areas and wells. Note the small grey symbols showing sinter deposits. Alteration appears orange-grey.

GEOPHYSICS

The prospect area has been the focus of resistivity surveys providing a widespread set of more than 100 audio frequency magnetotelluric soundings (AMT) and a more focused set of 22 time-domain electromagnetic soundings (TDEM) (Figure 3). Low, long period signal strength during the survey and local electrical noise limited the application of a full magnetotelluric survey in the area (Cumming, 2009).

High conductance through the local AMT depth limit of about 400 m occurs along the thermal trend with concentrated areas around the northern and southern fumaroles (Figure 3). Another part of the conductance anomaly extends to the south on the western flank of the stratovolcano. The resistivity data do not cover the summit of Tolhuaca due to difficult access. Argillic alteration mapped at the surface and in the wells confirms that argillic alteration is the primary cause of the conductor near the thermal areas.

A combination of the TDEM and AMT data sets at shallow levels reveals a widespread, persistent, roughly flat lying, thin resistive zone at about 100 m depth within the conductor (Wilmarth et al, 2011) (Figure 4). This resistor correlates precisely with a zone in the Tol-1 well that shows relatively high temperature mineralization. This zone produced

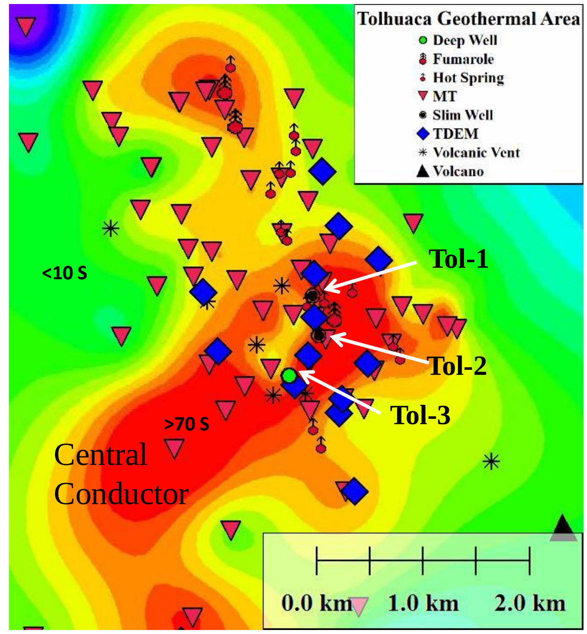

Figure 3: Total Conductance to 400 m depth. The central conductor is consistently over 70 Seimens. The resistive hole persists through this depth range in an area west of the wells.

steam from an aquifer at about 170°C based on the maximum flowing steam pressure during the test. The altered steam zone was confirmed in a higher pressure well kick at the same depth while drilling Tol-2 and intense alteration and high temperatures observed in the shallow portion of Tol-3.

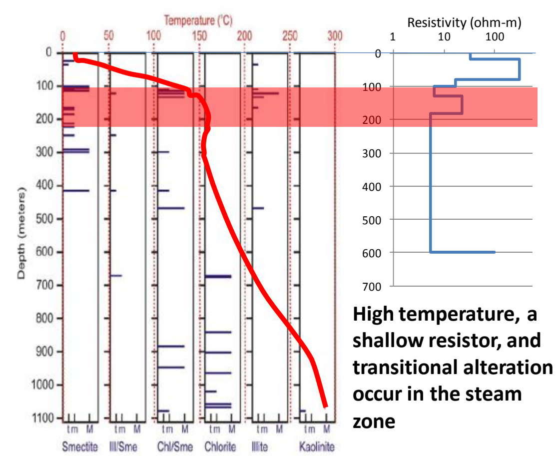

Figure 4: Secondary mineralization in Tol-1 shows chlorite-smectite, illite-smectite, and illite in a zone with high temperature and a nearby shallow resistor from TDEM data. This zone produced steam in the well test at Tol-1

The central conductor in the AMT data has a persistent resistive hole through the limited depth range of the data (Figure 3). If the thin-flat resistor in Figure 2 and central-resistive anomalies are related, the resistive hole could represent an area with a relatively high temperature history. This area is a likely candidate for the location of a shallow upflow zone.

DEEP WELL GEOLOGY

The two slim wells encountered interbedded flows, breccias, volcaniclastic deposits, tuffs, and dike rock through their total depths. The alteration varies from weak to intense and is typically stronger in tuffs and breccias compared to the lavas and dikes (J. Stimac, pers. com., 2011). Thin section and XRD analyses of Tol-1 (Moore, 2010) show an upper zone of argillic alteration (20 to 450 m), a transitional phyllic zone (450 to 650 m), and a deeper zone of propylitic alteration (650 + m). Within the shallow argillic alteration zone, rocks between 100 and 165 m contain a higher temperature transitional alteration assemblage that includes both illite and mixed layer illite-smectite (Figure 4).

The most intense alteration is focused in the shallow zone and at depths below about 500 m. Core studies of Tol-1 included rock oxygen isotope analyses of samples collected along the wellbore (Figure 5) (Winick, 2009). Similar to the observations of alteration intensity, the isotopes show two zones with relatively low (more-exchanged) values at 100 to 165 m depth and a broader more-exchanged zone at depths below 500 m with an intervening less altered zone of low apparent permeability.

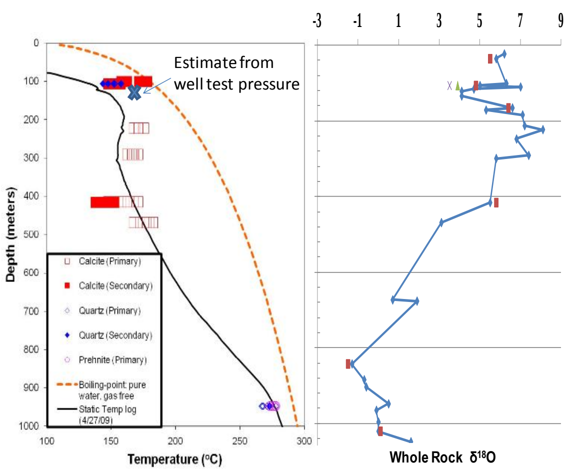

Figure 5: Well and fluid inclusion temperatures compared to whole rock oxygen isotope ratios.

Core observations revealed several hydrothermal breccias at depths ranging from 100 to 950 m (Figure 6). Hydrothermal breccias have also been found in cuttings at shallow levels in Tol-3 from about 100 m through 400 m. Samples of breccias as shallow as 100 m depth and outcrop of an intensely altered breccia containing vein fragments in the drilling area suggest that hydrothermal eruptions may have occurred.

Figure 6: Hydrothermal breccia in core from Tol-1 at 102 m depth.

Study of the thin sections, fluid inclusions, and XRD analyses from the core at Tol-1 showed that the system proceeded through four phases (Moore, 2010). Moore's report is followed closely in the remainder of this section. Fluid inclusion temperatures are shown in Figure 5.

The earliest stage represents an initial episode of heating (stage 1). Smectite, interlayered chlorite smectite and zeolites were deposited in the argillic zone. Interlayered chlorite-smectite was deposited in the phyllic zone and epidote and chlorite precipitated in the propylitic zone.

The formation of the geothermal system was followed by an episode of widespread boiling (stage 2). Boiling resulted in the formation of amorphous silica, chalcedony and quartz in the argillic zone and chalcedony, quartz, bladed calcite and hydrothermal brecciation in the propylitic zone. The deposition of multiple silica polymorphs (amorphous silica and chalcedony) is unusual in geothermal reservoirs and suggests significant rapid depressurization.

The third stage is represented by cooling and an influx of bicarbonate-rich steam-heated waters. Heating of downward percolating waters resulted in the precipitation of late-stage calcite as vug fillings throughout the upper 900 m of the well and sporadically at greater depths. Below 900 m depth, cooling favored the formation of prehnite after epidote. Occasional wairakite deposition followed the formation of prehnite and was the last mineral to form. It precipitated where steam-heated waters mixed with in-situ reservoir fluids.

In stage 4 temperature increases were recorded by fluid inclusions trapped in calcite at intermediate depths, and possibly by quartz and prehnite near the base of the well. At some stage calcite was deposited at shallow depths with a coating of fine grained bladed calcite consistent with influx of secondary bicarbonate waters that subsequently boiled.

WELL TEST DATA

The two deep slim wells reveal the presence of a shallow hot aquifer (Figure 7). Tol-1 produced dry steam from depths between 116 and 161 m depth during an interim rig test. The maximum flowing pressure in that test suggested a stable formation temperature in this zone of about 170°C (Figure 5). Tol-2 produced dry steam in a well kick from near the same elevation. Tol-3 shows the influence of the same zone in the temperature logs and alteration. This shallow zone correlates with high temperature mineralization and the resistive interval defined by the TDEM data. In both slim wells this zone was later cemented. Final cemented casing was set at 503 m in Tol-1 and 293 m in Tol-2 in. Shallow temperatures in water wells and the abundant hot springs are consistent with a hot shallow aquifer that has an extent similar to the extent of the central conductor (Figures 2 and 3).

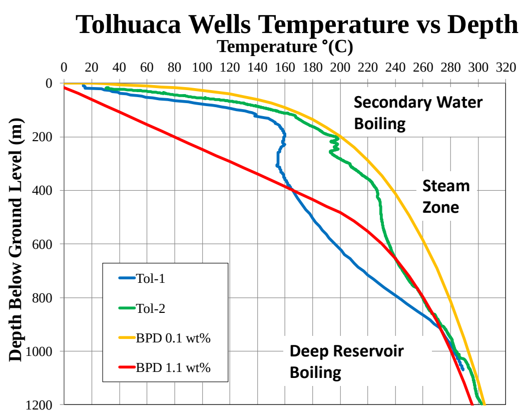

Figure 7: Tol-1 and Tol-2 temperature-depth profiles with Boiling Point vs Depth curves for hydrostatic pressure conditions and gas contents of 0.1% and 1.1%. Deep temperatures show reservoir liquid boiling conditions. Shallow temperatures show secondary liquid boiling conditions. Intermediate depth temperatures indicate steam-dominated conditions for estimate reservoir gas content.

The shallow steam zone shows a strong decline in pressure and temperature from Tol-2 to Tol-1 across 375 m of lateral separation. Steam pressures decline from 18 to about 9 bars and temperature from almost 200 to 170°C between the two wells. This decline occurs in spite of the apparent continuity of the aquifer from temperature, permeability, and mineralization information and confirmation of a continuous thin resistor reflecting high temperature mineralization at that depth from the TDEM data.

During a short flow test following well completion, Tol-2 vigorously produced single phase liquid to the surface. The hole was open from 293 to 1274 m. The well could only be tested briefly at about 5% total valve opening due to limited test facilities and well control issues. The wellhead temperature, pressure, and flow rate increased constantly upon each opening of the well for a period of several minutes until the well was shut in at the safe operating limit. The Tol-2 testing produced about 1.5 wellbore volumes.

The temperature profiles near the bottom of all three wells is consistent with a boiling point vs. depth (BPD) curve calculated at hydrostatic pressure and the 1.1% gas content in the total flow measured in the test samples from Tol-2 (Figure 7). (Fluid chemistry is described below). Between 600 and 200 m depth, temperatures in Tol-2 are above the hydrostatic 1.1% gas BPD curve suggesting steam-dominated conditions nearby. At shallower depths in both wells, the temperatures are near the BPD curve for low gas water. The temperature in this depth range may be controlled by slow influx and boiling of low gas steam-heated water.

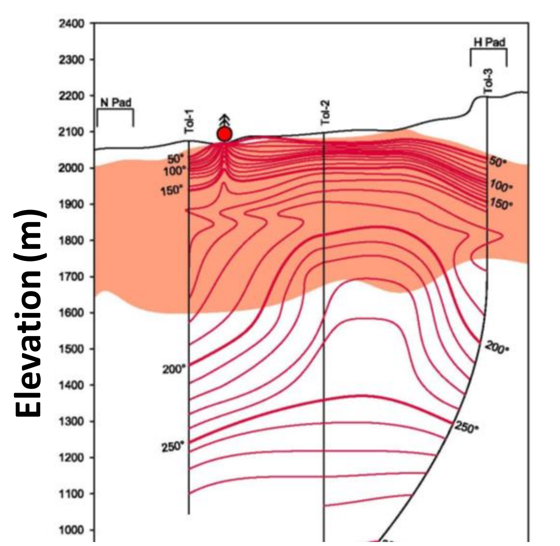

Figure 8: Schematic cross-section showing measured temperatures interpreted to be consistent with a nearby upflow zone (Wilmarth, pers.com., 2011).

FLUID GEOCHEMISTRY

Fluid chemistry samples include the hot spring liquids, the liquids from the Tol-2 well test, the fumarole gases, and the gases from the well tests.

The hot springs demonstrate the occurrence of a low-temperature steam-heated aquifer over the central part of the prospect. Chemical evidence of steam heating includes high bicarbonate and relatively high boron compared to chloride. The hottest springs discharge liquids with 1500 ppm bicarbonate and CO_2 at about 60°C.

The liquid samples from the Tol-2 well test suffered from limited clean-up of drilling mud due to the short period of testing, although very little if any circulation was lost while drilling. Mud chemistry prior to the test included a chloride content of about 1000 ppm. This mud was flushed with fresh water from the well prior to the test. The high pressure sampling condition during the test indicated that the samples were collected from single-phase liquid at the surface. The chemistry was quite different between the early and late liquid samples. The initial sample was dilute. The sample taken at the end of the test showed strong increases in bicarbonate, chloride, and silica up to 462 ppm. Although the early sample was clearly impacted by mixing with drilling mud and fresh water, the increased concentrations of silica and the limited mud losses while drilling support the likelihood that reservoir liquids contributed strongly to the second sample. However the liquid chemistry of these samples is not considered reliable.

The fumarole and well gases fall into two groups (Table 1). Group 1 includes the samples from the shallow Tol-1 well test and the nearby southern fumarole (Figure 2). Group 2 includes the deep production sample from Tol-2 and the northern fumaroles.

Table 1: Selected gas composition in mole%. The wells are T1 and T2. The other samples are from fumaroles.

	CO2	H2S	NH3	Ar	N2	CH4	H2
Group 1							
M	93.2	2.7	.011	.0028	1.87	.013	2.19
T1	94	.55	.05	.0053	3.01	.018	2.39
Group 2							
S	80.1	11.2	.033	.0103	1.42	.542	6.74
G	83.1	7.88	.03	.014	1.63	.613	6.78
T2	79.3	5.27	3.12	.0231	1.67	2.42	4.33

Group 1 gases show relatively high nitrogen-argon ratios (Figure 9), low methane, and high hydrogen contents. Group 2 is characterized by moderate nitrogen-argon ratios, higher argon, higher methane, higher hydrogen sulfide, and high hydrogen contents. Drilling materials may have affected the methane level in Tol-2. Helium isotope data show marginally higher ratios in the Group 1 samples, although both groups have ratios near 7 R/Ra. Comparison of gas chemistries on standard gas plots (Powell and Cumming, 2010), suggests that Group 1 gases contain a greater component of magmatic gases (Figure 9), have higher geothermometer temperatures (Figure 10), and perhaps reflect more oxidized conditions (higher carbon dioxide with lower methane and hydrogen sulfide). Group 2 shows a greater contribution of air-saturated meteoric water and lower geothermometer temperatures.

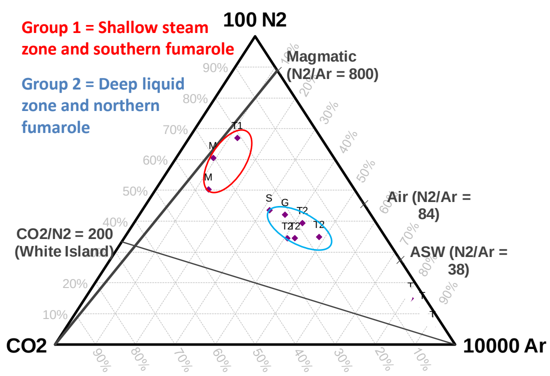

Figure 9: CO2, N2, Ar Ternary Plot shows the two groups of gases. The shallow sample from Tol-1and the samples from the southern fumarole show stronger magmatic influence.

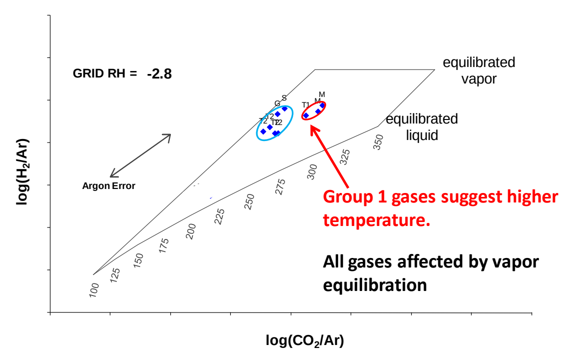

Figure 10: H2/Arv s. CO2/Ar plot from Giggenbach suggesting that the Group 1 (shallow-southern) gases record a higher reservoir temperature. Both groups show elevated hydrogen relative to liquid equilibrium.

The methane in Group 2 is consistent with the approach to Fisher-Tropsch equilibrium or stronger organic contributions. High hydrogen contents in both groups suggest that vapor phase equilibration may be in progress.

In summary the chemistry appears to record the presence of a deep, high temperature liquid reservoir with a relatively strong meteoric component, some suggestion of steam phase equilibration, and relatively high organic contributions or generation of geothermal methane. These gases imply a connection of the deep system at Tol-2 to the surface at the fumaroles to the north. The deep liquid reservoir is overlain by a shallow steam zone that shows a stronger magmatic influence and is less equilibrated or has a lower organic contribution. Steam-heated bicarbonate liquids occur above and perhaps laterally marginal to the steam zone.

CONCEPTUAL MODEL

A conceptual model of the Tolhuaca geothermal reservoir is shown in Figure 11. The main features of the geothermal system are a deep liquid upflow near Tol-2, influx and mixing of meteoric water from the northwest at depth, and a shallow steam-dominated reservoir.

The resistive center of the central conductor may represent the shallow part of an upflow zone that feeds the two reservoir levels. In this case the resistive hole in the conductor would be due to relatively high temperature transitional-phyllic mineralization similar to the surrounding thin horizontal resistor and in contrast to the more persistent argillic alteration seen in the wells.

The upflow zone feeds the deep boiling reservoir. This fluid is then mixed with aerated groundwater and undergoes geothermal re-equilibration. The aerated groundwater end-member may circulate fairly deep from lower elevation sources to feed the high pressure reservoir. The temperatures at depth in the wells are controlled by boiling of this high-gas mixed reservoir liquid.

Continued upflow from depth becomes steam-dominated as suggested by the Tol-2 temperature interpretation, bypasses the low permeability, relatively un-mineralized section from 200 to 500 m depth in Tol-1, and then feeds the shallow steam zone.

The shallow steam zone may have originated as a near-boiling roughly horizontal liquid aquifer during the early stages of system development. This aquifer fed the silica hot spring terraces and generated an extensive shallow, flat and thin electrically resistive zone. Fluid inclusions record temperatures near the boiling point for pure water in this aquifer.

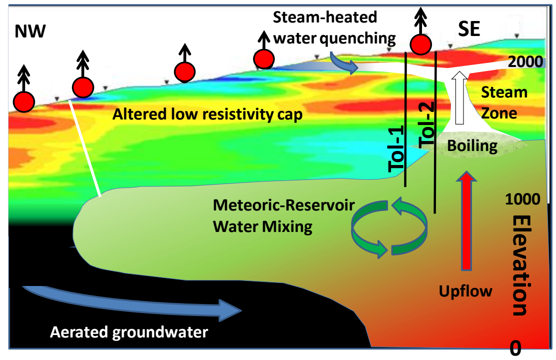

Figure 11: Conceptual cross-section of the Tolhuaca Reservoir shown with various interpreted processes labeled on the figure.

Hydrothermal breccias, vapor-rich fluid inclusions, amorphous silica and bladed calcite formed during periods of boiling. Evidence of boiling extends to depths of about 950 m depth and may have been associated with hydrothermal eruption. As the pressures dropped, the reservoir was invaded by dilute, steam-heated meteoric water. This event was recorded by fluid inclusion temperatures significantly below the boiling point curve for pure water and the deposition of calcite.

Measured temperatures that are greater than the lowest fluid inclusion temperatures document subsequent re-heating. Ultimately the renewed high temperatures established the present-day two level reservoir with steam and steam-heated waters at shallow depths and a deep liquid reservoir below. Oxygen isotope values in Tol-1 between these zones suggest limited water-rock interaction and low permeabilities throughout the life of the system at Tol-1 in the intermediate depth zone.

The shallow steam zone appears to be quenched as it extends away from the upflow such that it eventually resolves into steam-heated liquids as seen in the hot springs. The shallow quenching process is evident in the pronounced loss of temperature and pressure in the shallow zone between the two slim wells and the steam-heated hot spring chemistry. The quenching may be caused by influx of steam-heated snow melt. The abundant winter and occasionally intense summer snow at Tolhuaca melts to a liquid with low gas content (due to low gas solubility in ice) such that the deep upflow gas chemistry could be preserved in the shallow samples in spite of mixing during the quenching/re-boiling process. The snow melt becomes slightly gas-charged as it becomes steam-heated bicarbonate water, invades and quenches the shallow steam zone. It may re-boil as suggested by the congruence of shallow measured temperatures with a low gas BPD.

REFERENCES

Cumming, W.; 2009; "Chile Exploration 2009"; Presentation to GGE; April 26, 2009.

Moore, J.; 2009; "A Petrologic and Fluid Inclusion Investigation of Selected Samples from GeoGlobal Energy LLC Well Tolhuaca 1*", EGI report to GGE*, Dec. 18, 2010.

Powell, T. and W. Cumming; 2010; "Spreadsheets for Geothermal Water and Gas Chemistry"; *Proc. Thirty-Fifth Workshop on Geothermal Reservoir Engineering* Stanford University, Stanford, California, February 1-3, 2010, SGP-TR-188

Wilmarth, M., Cumming, W., Melosh, G., Sussman, D., and Stacey, R.; 2011; "A Resistive Donut Hole Interpreted as a Shallow, Fractured, Vapor-Dominated Geothermal Reservoir"; AGU abstracts,

Winick, J.; 2010; "2009 Tolhuaca Sampling and Analysis Program"; GGE report; March 10, 2010.

Stacey, R.; 2011; "Tol-1 and Tol-2 Temperature and Pressure Profile Interpretation"; GGE report, Date: November 14, 2011, Nov 14, 2011.